

HIGH AVERAGE POWER UV FREE ELECTRON LASER EXPERIMENTS AT JLAB*

David Douglas[#], Stephen Benson, Pavel Evtushenko, Joseph Gubeli, Carlos Hernandez-Garcia
Robert Legg, George Neil, Thomas Powers, Michelle Shinn, Chris Tennant, and Gwyn Williams
Jefferson Lab, Newport News, VA 23606, USA

Abstract

Having produced 14 kW of average power at $\sim 2 \mu\text{m}$, JLAB has shifted its focus to the ultraviolet portion of the spectrum. This contribution describes the JLab UV Demo Free Electron Laser (FEL), presents specifics of its driver energy recovering linac (ERL), and discusses the latest experimental results from FEL experiments and machine operations.

HISTORY AND CONTEXT

The successful operation in August 2010 of visible-wavelength (700 nm and 400 nm) high-power continuous wave (CW) FELs at Jefferson Lab was the culmination of an effort spanning more than 20 years. The potential of superconducting radio-frequency (SRF) linacs as drivers for short wavelength FELs was immediately recognized during construction of CEBAF [1], and a design for a CEBAF-driven FEL rapidly developed. Means of CEBAF operation for simultaneous nuclear physics and FEL use were devised [2], and by 1993 the commissioning of CEBAF was proceeding with portions of an FEL injector in place, integrated with the primary nuclear physics system through use of a “nuclear physics bypass” [3].

Progress was, however, funding limited. In parallel, accelerator and FEL technology, the science case for a high-power, short-wavelength CW FEL, and user enthusiasm rapidly evolved. These influences combined to motivate the design (beginning as early as 1991 [4]) of a series of stand-alone systems that laid the foundation for subsequent efforts at JLab. These efforts culminated in the “Industrial Prototype” FEL [5], which was configured to provide kW powers across the spectrum from IR to UV and invoked the use of an ERL as a means of cost control. The system concept supported both basic science research and industrial applications such as micromachining and materials processing [6].

The promise of this concept was sufficient to garner funds from the Commonwealth of Virginia for a facility to house it (Figure 1). The availability of this site leveraged funding for a system (and constrained future use, as discussed below); shortly thereafter, the Office of Naval Research funded construction of a sequence of successful SRF ERL driven high power infrared (IR) FELs: the IR Demo [7] (2.3 kW in 2001 [8]) and the IR Upgrade [9, 10, 11] (14.3 kW in 2006). In addition to generating record CW power, the latter system forms much of the

basis of the system now under discussion: coincident with funding of the IR Upgrade, the US Air Force provided initial support for the construction of a UV FEL in the same facility, using – insofar as possible – the same hardware.

As with the legacy CEBAF-based system, progress was funding-limited, but through a sequence of awards from various sources the installation of a system comprising an SRF ERL driven oscillator FEL was completed in 2010. Initial operation in the visible with wavelength reach (through coherent harmonics) to the VUV was immediately realized; user operations continue to date.

FEL CONCEPT AND DESIGN

System Concept

Since the advent of the “stand-alone system” [5], this “UV Demo FEL” has been an SRF ERL-driven oscillator with modest single bunch energy, but providing extremely high average power *via* the high repetition rate of the superconducting driver. The utility and cost effectiveness of this architecture has been recognized for over two decades [12], and the use of low bunch charge to provide optimal beam brightness and FEL performance validated by IR Demo and IR Upgrade experience.

Two constraints are imposed by early design choices. Firstly, the system is based on an APS Undulator A, a demonstrated and commercially available design. The elevation of this device – 1.4 m – must be reconciled with the JLab standard beamline height of ~ 0.7 m. This difference is resolved by a feature of the legacy design – the availability of a ~ 1 m deep pit in which the wiggler could be placed and thereby matched to the beamline elevation. Thus a second constraint emerges: the electron beam transport must utilize the pit location provided in the pre-existing facility (Figure 1).

FEL Design Details

The as-built system [13] utilized an APS Undulator A prototype on loan from Cornell University. Though largely identical to the production wiggler, the prototype is shorter by 12 periods, leading to minor changes in details of the legacy design [6]. The optical cavity is an evolution of the 32 m design used in the JLab IR Upgrade [14], and incorporates lessons learned from high power operation. Optical cavity and electron beam design parameters are presented in Table 1. While the resonator is near-concentric, the wiggler is displaced toward the

* Notice: Authored by Jefferson Science Associates, LLC under U.S. DOE Contract No. DE-AC05-06OR23177. The U.S. Government retains a non-exclusive, paid-up, irrevocable, world-wide license to publish or reproduce this manuscript for U.S. Government purposes.
#douglas@jlab.org

high reflector. The mirror substrates are single crystal sapphire, coated with ion-beam sputtered coatings.

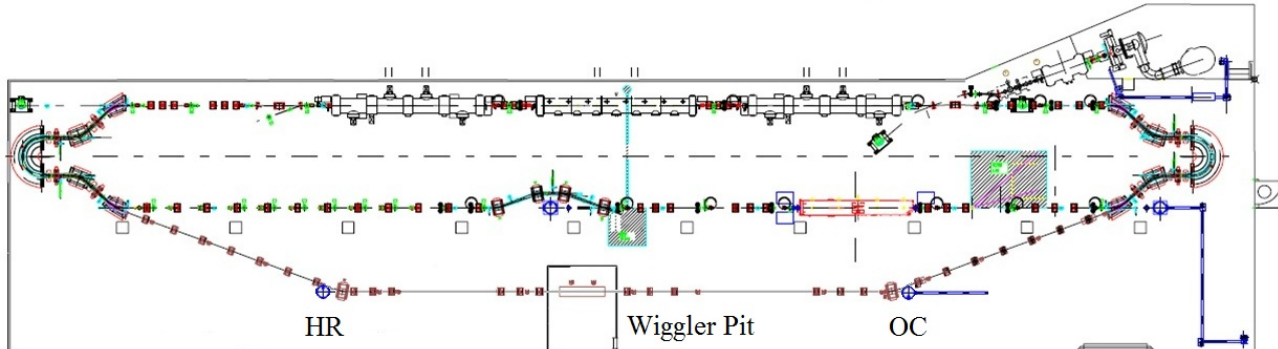


Figure 1: JLab IR and UV FELs in facility. Top beam line: SRF linac; middle: IR recirculator; bottom: UV recirculator. UV High Reflector vacuum vessel (HR): lower left; Wiggler pit: bottom center; UV Out-Coupler (OC): lower right.

Table 1: UV Demo FEL Design Parameters

Cavity length (m)	32.04196
Mirror radii (cm)	2.54
High reflector radius of curvature (m)	14.43±0.02
Output coupler radius of curvature (m)	17.72±0.02
Wiggler period (cm)	3.3
Number of periods	60
K_{rms}	0.816
Emittance (microns)	5
α_x, α_y	1.25, 0.77
Beam radii (σ_x, σ_y)	196, 175
Energy spread (%)	0.3
Full pulsewidth (fs)	450
Bunch charge (pC)	60
Peak current (A)	200

Mirrors are water-cooled, but cryo-cooling can be implemented. Each cavity vacuum vessel accommodates four mirrors to allow wavelength agility. At present, installed mirrors allow lasing in bands around 372nm, 400nm, and 700nm. The shortest wavelength uses hole outcoupling; the others are transmissive ($R = 90 \pm 0.5\%$).

Design analysis [13, 15] was conducted using a spreadsheet implementation of 1D formulae by Dattoli [16, 17] and with a pulse propagation code based on Colson’s formulae [18]. These models agreed favourably (20%) with gain and power results from our IR FELs. The high IR gains ($\sim 100\%$) pushed the codes to the limits of their applicability; for the UV Demo FELs the anticipated gains appeared higher still, so performance was also modelled with the 3D Wavevnm code developed at the U.S. Naval Postgraduate School (NPS) [19]. In all cases, results were encouraging and consistent, with predicted net gains over 70% and extraction efficiencies of 0.5% (pulse propagation code) to 0.7% (spreadsheet and 3D

code), relatively close to the rough scaling $\frac{1}{2}N_w = 0.83\%$. Detuning curves predicted by 1D and 3D models were $\sim 4\text{-}5 \mu\text{m}$. A comparison of these design projections with observations and detailed FEL modelling is made below.

Experience with the IR FELs indicated that mirror heating from absorption of internal cavity power and of THz radiation generated by bending the fully compressed bunch off of the optical cavity axis (just upstream of the out-coupling optic “OC”, in Figure 1) would cause mirror distortion and preclude scaling of projected performance to high powers. Estimates of these effects suggested that output powers would be limited to $\sim 100 \text{ W}$ during CW operation unless cryogenic mirrors were utilized.

DRIVER ERL

The UV driver ERL [20] shares the linac and portions of a recirculator with the IR Upgrade driver [9, 10, 11]. It is, however, a distinct system with respect to operating parameters and beam handling configuration.

Design Requirements

The ERL is subject to several requirements. It must deliver to the wiggler an electron beam with phase space configured so as to optimally drive the FEL interaction (see Table 1), and then energy-recover the large-energy-spread FEL exhaust beam. These primary tasks must be accomplished while preserving beam quality, controlling instabilities, and avoiding excessive loss from the high power CW beam. A legacy design feature imposes a third constraint: the available wiggler has a 1.4 m elevation, forcing use of a pre-existing “wiggler pit” to lower the mid-plane to JLab-standard beam line elevation ($\sim 0.7 \text{ m}$); this pit is offset $\sim 5 \text{ m}$ from the IR system (Figure 1).

Implementation

Geometric requirements are met by using a feature supplied in IR Upgrade transport dipoles in anticipation

of UV construction: the corner dipoles [21] of the transport can be “switched” to direct the beam to/from a bypass beamline. For UV operation, they operate at half their IR field, halving the bend angle at the end (beginning) of the IR delivery (recovery) arc. The reduction in angle directs beam toward the pit; the bend onto (off of) the axis of the optical cavity is completed achromatically through use of a FODO-focusing transport managing dispersion, controlling beam envelopes, and allowing chromatic correction with sextupoles.

Delivery of the optimal beam to the wiggler and its recovery thereafter requires both transverse and longitudinal phase space matching during acceleration, transport to the wiggler, and energy recovery. Multiple quadrupole telescopes bridge sub-regions of the machine (injector, linac, arc, bypass, wiggler, return bypass, arc, linac second pass) and allow betatron matching with sufficient operational flexibility to meet all constraints.

As the UV system shares Bates arcs with the IR, the longitudinal match [22, 23] is both robust and flexible. This process has three unique features. First, compression is performed using arc momentum compactions; there is no compressor chicane. This allows, secondly, full compression with acceleration on either side of crest of the RF waveform; operation is not restricted to the rising side. Thirdly, linearization of RF curvature effects is performed with the transport system sextupoles (and, for energy compression required for lossless recovery, using octupoles as well); harmonic RF is not used or needed.

Features common to the IR and UV ERLs are evident from Figure 1 and include injector, linac, and dump beam lines in addition to the Bates bends. A comparison of achieved performance is given in Table 2.

Table 2: Comparison of Achieved System Parameters

Parameter	IR	UV
Energy (MeV)	88-165	135
I_{ave} (mA)	9.1	5
Q_{bunch} (pC)	135	60
$\mathcal{E}_N^{transverse}$ (mm-mrad)	8	5
$\mathcal{E}_N^{longitudinal}$ (keV-psec)	75	50
$\sigma_{\delta p/p}, \sigma_l$ (fsec)	0.4%, 125	0.35%, 100
I_{peak} (A)	400	250
FEL rep rate (MHz) (32 m optical cavity fundamental = 4.678 MHz)	0.58-74.85	1.17-74.85
η_{FEL}	2.5%	0.7%
ΔE_{full} after FEL	~15%	~7%

Beam Dynamical Issues

The large FEL exhaust energy spread leads to concerns with transport system aberrations. These are managed by keeping beam envelopes and quadrupole strengths at modest magnitudes, and by controlling evolution of phase advance through the system (to suppress aberrations *via* constructive interference). Sixteen sextupoles in seven families provide control of nonlinear dispersion and path length variation with momentum (T_{566}).

Collective effects differ in character from those in the IR ERL. Lower bunch charge alleviates space charge effects – improving beam brightness – and reduces average current – mitigating instabilities and interaction of the beam with the environment. Thus, for example, we can adequately control beam break up (BBU) by choice of pass-to-pass phase advance, in contrast to use in the IR ERL of a horizontal/vertical phase space exchange.

Management of coherent synchrotron radiation (CSR) effects is informed by experience with the IR [10, 20]. Low bunch charge alleviates CSR-induced beam quality degradation, but THz-loading-driven mirror heating is a limitation. As noted above, mirror distortion due to such heating limits output power to ~100 W. This can, in principle, be mitigated as in the IR Upgrade [10] by use of a THz management chicane [24, 25] (installed in a slot available downstream of the wiggler), THz traps, and cryogenic mirrors in the optical cavity.

INSTALLATION AND COMMISSIONING

Installation and commissioning [26] were constrained by funding profiles and priority operation of the IR FEL; these limitations were addressed using phased scheduling of IR operation and UV installation and commissioning.

Initial funding from the AFRL allowed fabrication of many UV components during IR construction, and permitted installation during IR maintenance periods. After operation of the IR FEL at over 14 kW in October 2006, the tempo of UV work increased. Incremental funding in 2007 led to a minimally instrumented system under vacuum by late 2009, allowing commissioning to start. The wiggler was in place but the jaws were fully open and a simple 3” round chamber in place. This minimized magnetic effects on the beam and provided substantial clear aperture, mitigating potential beam loss and limiting exposure to beam loss.

A chronology is given in Table 3. Delays in component fabrication were addressed by configuring the driver ERL for short beam test runs, allowing integration of hardware as it became available. Nominally a work-around, this approach had the beneficial effect of focusing activities to limited segments of the system at any given time.

Table 3: Installation and Commissioning Milestones

Activity/ <i>Milestone</i>	Dates (mm/dd/yy)	Incremental Beam Time
IR operations; design, fabricate, install	01/01/03- 10/27/09	
<i>initial beam operations</i>	10/28/09	
<i>1st beam to dump</i>	10/28/09	2.5 hours
transport installation, IR operations	10/29/09- 07/01/10	n/a
commission ERL	07/02-07/10	
install FEL diagnostics	07/08-20/10	
commission ERL	07/21-30/10	
<i>1 mA CW beam to dump</i>	07/29/10	+100 hours (+13 shifts)
install wiggler chamber	08/01-16/10	
commission 700 nm	08/17-23/10	
<i>1st light, 700 nm</i>	08/19/10	+32 hours (+ 4 shifts)
<i>150 W CW at 700 nm</i>	08/19/10	+ 3 hours
site utility down	08/24-26/10	
commission 400 nm	8/27-31/10	
<i>1st light, 400 nm</i>	08/31/10	+37 hours (4 shifts)
<i>104 W CW at 400 nm</i>	08/31/10	+3 hours
<i>10 eV 3rd harmonic</i>	12/19/2010	

Though driven primarily by cost and schedule constraints, the relatively rapid transition (in hours of beam operation) from high power IR operation to shorter wavelengths validated this use of phased installation, commissioning, and operation. Of particular value were the close coupling of IR and UV system hardware designs and the use of shared hardware. Common subsystems had been in operation for IR and were reliable and well optimized; use of similar hardware in independent subsystems provided a knowledge and experience base that made diagnosis and correction of problems rapid and inexpensive.

Following extensive runs to characterize the FEL during operation at visible wavelengths, harmonic operation was tested. CW VUV coherent third harmonic output at 124 nm (10 eV) was extracted in December 2010 through use of a hole-coupled FEL out-coupler during operation at the 372 nm fundamental. As expected, the third harmonic intensity was $\sim 1/1000^{\text{th}}$ that of the fundamental, with power at the mW level. Details are given in [26]. Figure 2 presents an image of the FEL optical cavity outcoupler during 400 nm operations

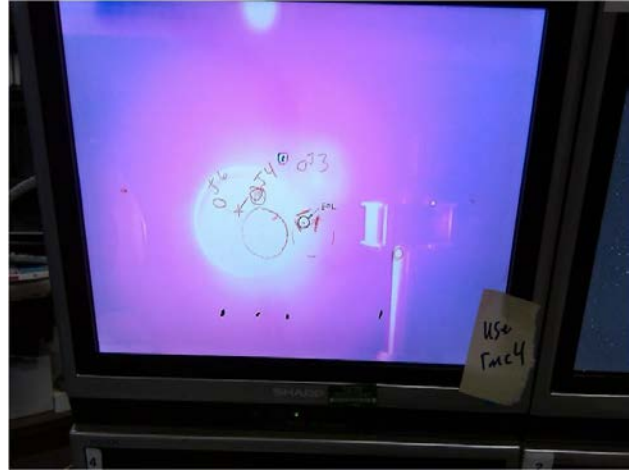


Figure 2: FEL outcoupler during 400 nm operation.

FEL PERFORMANCE

Experience with the JLab IR FELs guided the design, fabrication, and commissioning of this system. When brought on line [13, 15] the design of optical cavity [14] and optical diagnostics – together with use of a relatively novel method for searching for resonant cavity length [26] – allowed rapid progress to first light (see Table 3).

Initial observations confirmed that the low power extraction efficiency was of order $\frac{1}{2}N_w$ and efficiency rolls off, as expected, with mirror loading (Figures 3 and 4). This led to the ~ 100 W output powers discussed above (Table 3). What was not anticipated were the observed extremely high gains (*e.g.*, Figure 5) and very long detuning curves (over 12 μm at 700 nm) that were observed. This motivated a systematic comparison of the experiments to the design analysis and to detailed simulations of FEL performance using multiple codes.

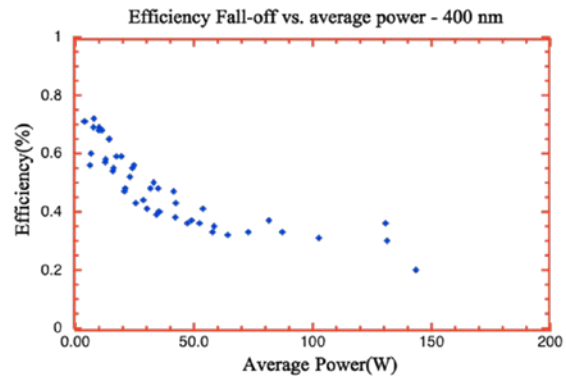


Figure 3: 400 nm lasing efficiency vs. power

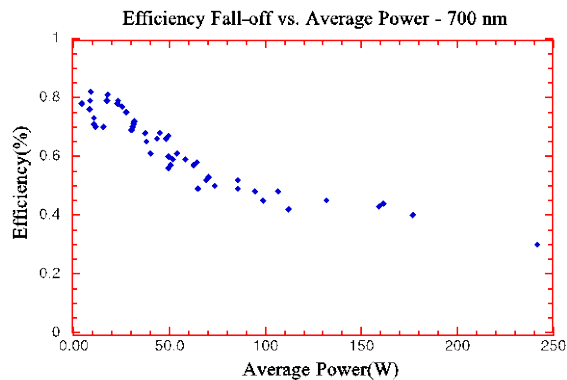


Figure 4: 700 nm lasing efficiency vs. power



Figure 5: FEL gain data acquisition software. Left: linear scale; right: logarithmic scale

These comparisons are summarized in Table 4. The results of simulation and analysis consistently fail to predict performance at the observed level: either gain, detuning curve length, or extraction efficiency (or some combination thereof) fall short of observation. No single model captures all observed details, but it clear that the system performance exceeds, in general, predictions in one or more relevant metric.

The performance of the UV FEL has greatly exceeded both 1D and 3D predictions; there is in no single case a fully consistent agreement of model with observation. This unusual circumstance is not yet understood, though it may possibly be due to an electron drive beam that is of “higher quality” than that so far characterized by our preliminary empirical studies.

As noted above, successful VUV operation was achieved at 10 eV using third harmonics generated while lasing at a 372 nm fundamental [26].

Table 3: Comparison of Models and Observations

<i>Parameter</i>	<i>Simulation</i>	<i>Experiment</i>
------------------	-------------------	-------------------

turn-on time	8.6 μ sec	5 μ sec
net gain	\sim 70%	\sim 150%
detuning curve	4.5 μ m	$>$ 7 μ m
efficiency	0.5-0.7%	0.73 \pm 0.05%
<i>Basis of Comparison</i>	<i>Net gain (%)</i>	<i>efficiency (%)</i>
JLab spreadsheet	75	0.7
Genesis/OPC (3D)	88	0.67
Wavenm (NPS-3D)	88	0.72
Medusa/OPC (3D)	119	0.63
Medusa/OPC (4D)	119	0.41
Experiment	145 \pm 10	0.73 \pm 0.05%

STATUS AND FUTURE DIRECTIONS

Facility operations (in both IR and UV) are fully funded for FY2012; at this writing the UV system is coming back on the air following a year-long shutdown, and on 10 May 2012 recovered lasing at 778 nm. Third harmonic VUV user service at 10 eV is imminent. In the next few years, system performance will be made increasingly robust through improvements to the driver and to the FEL itself. Initial funding is available for a new electron gun and to refurbish linac SRF systems. With higher operating voltage, the new gun will provide better beam brightness and mitigate challenges associated with high current operation; higher linac energy will move the FEL fundamental wavelength reach into the near UV. The addition of cryogenic optical cavity mirrors will reduce constraints imposed by mirror loading and allow operation at kW levels in the visible and UV.

An intriguing proposed application of the driver ERL repurposes it for use with an internal target to search for dark matter. The “DarkLight” experiment [27] will interact the e^- beam with a hydrogen gas jet \sim 20 cm in length in a circular aperture of 2 mm diameter. Beam quality and beam halo control are of critical importance, and will undergo validation testing in summer 2012.

Jefferson Lab is exploring options to move to even shorter wavelengths through upgrades to the existing facility [28], through a return to the legacy “CEBAF driver” concept [29], or through construction of a green field device [30]. In each case, the goal is to move to progressively shorter wavelengths (through use of brighter sources and higher energy), higher power, and expanded user operations. The available infrastructure and attendant knowledge base offer significant potential for very high performance in the UV and beyond.

ACKNOWLEDGMENT

This work would not have been possible without the active participation of all members of the JLab FEL team. We would, in addition, like to thank Mr. Stephen

Corneliusson of Jefferson Lab and Dr. Catherine Westfall of MSU for discussions on and assistance with the content and presentation of this material. Support was provided by of the Commonwealth of Virginia, the US AFRL, and the US DoE. This report was authored by Jefferson Science Associates, LLC under U.S. DOE Contract No. DE-AC05-06OR23177. The U.S. Government retains a non-exclusive, paid-up, irrevocable, world-wide license to publish or reproduce this manuscript for U.S. Government purposes.

[30] C. Tennant *et al.*, IPAC'11, San Sebastian, September 2011, THPC105, pp. 3134-6 (2011).

REFERENCES

- [1] G. Krafft and J. Bisognano, PAC'89, Chicago, March 1989, pp. 1256-8 (1989).
- [2] J. Bisognano *et al.*, , NIM A318, pp. 216-20 (1992).
- [3] G. Neil *et al.*, CEBAF-PR-92-029, August 1992.
- [4] D. Douglas *et al.*, CEBAF-TN-91-071, 12 September 1991.
- [5] G. Neil *et al.*, NIM A358, pp. 159-62 (1995).
- [6] H.F. Dylla *et al.*, PAC'95, Dallas, May 1995, pp.102-4 (1995)
- [7] G. Neil *et al.*, Phys. Rev. Lett. 84, 662-665 (2000).
- [8] G. Neil, PAC'03, Portland, May 2003, pp. 181-5 (2003).
- [9] C. Tennant, PAC'09, Vancouver, May 2009, TH3PB103, pp. 3125-9 (2009).
- [10] S. Benson *et al.*, PAC'07, Albuquerque, June 2007, pp. 79-81 (2007).
- [11] D. Douglas *et al.*, PAC'01, Chicago, June 2001, pp. 250-3 (2001).
- [12] R. Rohatgi, H. Schwettman, and T. Smith, PAC'87, Washington, March 1987, pp. 230-2 (1987).
- [13] S. Benson *et al.*, "Beam Line Commissioning of a UV/VUV FEL at Jefferson Lab", to appear in Proc. FEL'11, Shanghai, August 2011, WEOC11.
- [14] M. Shinn *et al.*, NIM A507, pp 196-9 (2003)
- [15] S. Benson *et al.*, PAC'11, New York, March 2011, THP171, pp. 2429-31 (2011).
- [16] G. Dattoli, L. Giannessi, and S. Cabrini, IEEE J. Quantum Electronics 28, 770 (1992).
- [17] G. Dattoli, *et al.*, NIM. A285 108, (1989).
- [18] W.B. Colson, Phys. Lett. 64A 190 (1977).
- [19] P.P. Crooker *et al.*, Phys. Rev. ST Accel. Beams 11, 090701 (2008).
- [20] D. Douglas *et al.*, PAC'11, New York, March 2011, THP173, pp. 2435-7 (2011).
- [21] D. Douglas *et al.*, JLAB-TN-03-015, 28 April 2003.
- [22] D. Douglas, BIW'10, Santa Fe, May 2010, WEIMNB02, pp. 506-15 (2010).
- [23] P.Piot *et al.*, Phys. Rev. ST AB 6, 030702 (2003).
- [24] D. Douglas, JLAB-TN-04-028, 16 September 2004.
- [25] S. Benson *et al.*, US Patent #7859199, 28 December 2010.
- [26] R. Legg *et al.*, PAC'11, New York, March 2011, THP172, pp. 2432-4 (2011).
- [27] J. Boyce, Proc. DSU2011, Beijing, September 2011.
- [28] C. Tennant *et al.*, PAC'11, New York, March 2011, THP187, pp. 2468-70 (2011).
- [29] A. Bogacz *et al.* SRI'03, San Francisco, August 2003, AIP Conf. Proc. 705, pp. 29-32 (2004).